
The Curse Revisited: a Newly Quantified Concept of Meaningful Distances for Learning from High-Dimensional Noisy Data

Robin Vandaele^{1,2,3}

Bo Kang³

Tijl De Bie³

Yvan Saeys^{1,2}

¹Department of Applied Mathematics, Computer Science and Statistics, Ghent University, Ghent, Belgium

²Data mining and Modelling for Biomedicine (DaMBi), VIB Inflammation Research Center, Ghent, Belgium

³IDLab, Department of Electronics and Information Systems, Ghent University, Ghent, Belgium

Abstract

Distances between data points are widely used in point cloud representation learning. Yet, it is no secret that under the effect of noise, these distances—and thus the models based upon them—may lose their usefulness in high dimensions. Indeed, the small marginal effects of the noise may then accumulate quickly, shifting empirical closest and furthest neighbors away from the ground truth. In this paper, we characterize such effects in high-dimensional data using an asymptotic probabilistic expression. Furthermore, while it has been previously argued that neighborhood queries become meaningless and unstable when there is a poor relative discrimination between the furthest and closest point, we conclude that this is not necessarily the case when explicitly separating the ground truth data from the noise. More specifically, we derive that under particular conditions, empirical neighborhood relations affected by noise are still likely to be true even when we observe this discrimination to be poor. We include thorough empirical verification of our results, as well as experiments that interestingly show our derived phase shift where neighbors become random or not is identical to the phase shift where common dimensionality reduction methods perform poorly or well for finding low-dimensional representations of high-dimensional data with dense noise.

ysis [Indyk and Motwani, 1998, Beyer et al., 1999, Aggarwal et al., 2001, Verleysen and François, 2005, Kuo and Sloan, 2005, Radovanović et al., 2009]. One such phenomenon is that the distances between data observation lose their usefulness. In particular, when our data is under the effect of *dense* noise—meaning that each of the true data entries is likely shifted by a small nonzero error value—empirical ‘neighbors’ (whether this means closest, k -nearest, furthest, ...) may be unrepresentative for ground truth neighbors. Unfortunately, noise is unavoidable in many real world data due to practical problems in the data collection and preparation processes [Zhu and Wu, 2004]. For example, biological data such as single cell sequencing data [Zhang et al., 2021] is often inherently noisy, due to the imprecise nature of biological experiments [Libralon et al., 2009]. Other high-dimensional examples include noisy images [Buades et al., 2005], and climate time series [Ertöz et al., 2003].

While noise may contribute little to individual dimensions, its overall contribution can be fatal for learning and inference if the data is high-dimensional. Intuitively, if the added *ground truth* (by which we mean *noise-free*) discrimination—this being how well we are able to differentiate between neighbors—with each added dimension cannot cope with this noise, closest and furthest points will become more random in nature. *Thus, if the ground truth model diameter does not sufficiently increase with the data dimensionality, (all) empirical neighbors lose their effectiveness under noise. Furthermore, it turns out that this may not always be effectively resolved by reducing our data dimensionality through common dimensionality reductions.* This is formally explored in this paper.

We emphasize that this is mainly a theoretical paper, in which we aim to provide further intuition into representation learning of high-dimensional point cloud data. We present and validate new theoretical results that complement previous work on *distance concentration*, discussed below. No concrete algorithms will

1 Introduction

Motivation In data science, *the curse of dimensionality* encompasses various phenomena occurring in high-dimensional data, which complicate their anal-

be presented, claimed, or suggested. Nevertheless, it is crucial to better understand and study the counter-intuitive phenomena of high-dimensional data in their own right, as this is imperative for one to be able to design better computational methods for their analysis.

Contributions

- We provide a probabilistic quantification of the effect of high-dimensional noise on neighboring relations, deriving conditions under which these relations either become highly random or non-random, independent of the magnitude of noise (Theorem 2.1 & Corollary 2.3).
- We provide thorough empirical verification of our theoretical results (Section 3.1).
- We use hyperharmonic series (Example 2.5) to develop experiments that directly link the performance of dimensionality reductions to the randomness of neighbors (Section 3.2).
- We conclude on how our work provides better understanding of representation learning of high-dimensional point cloud data (Section 4).

Related work It is no secret that many common distance measures lose their usefulness for discriminating between points in high-dimensional data. This phenomenon has been well studied on both a theoretical and experimental level by [Beyer et al., 1999], and consecutively by [Aggarwal et al., 2001, Durrant and Kabán, 2009, Kabán, 2012, Giannella, 2021]. The emphasis of this entire work is on the so-called *distance concentration* phenomenon, which is when distances become nearly indiscernible in high-dimensional data. “In other words, virtually every data point is then as good as any other, and slight perturbations to the query point would result in another data point being chosen as the nearest neighbor” [Beyer et al., 1999]. Hence, distance concentration is commonly regarded as indicative for distances being meaningless and unstable.

In this paper, we maintain an entirely different view of when distances are meaningful. We assume the common practical case that our observed data is composed of a *ground truth* component \mathbf{X} , and a (*dense*) noise component \mathbf{N} . We regard distances meaningful when our (closest, furthest, k -nearest, ...) neighborhood relations derived from our observed data $\mathbf{X} + \mathbf{N}$ likely coincide with those that would have been obtained from \mathbf{X} , and hence, are informative for the ground truth model underlying our data. Although this is a highly natural albeit different way to characterize the meaningfulness of distances in data, to the best of our

knowledge, a formal probabilistic analysis thereof is lacking.

It should come as no surprise that unlike distance concentration, our required conditions for distances to be meaningful will be difficult to assess in practice. Nevertheless, it is important to realize—as we show in this paper—that distance concentration is not effective for measuring this new notion of meaningfulness of distances. Indeed, through our results we are able to construct examples where even when distance concentration occurs, the inferred empirical neighborhood relations are still likely true, and remain so over different noise replicates.

Finally, dimensionality reductions are commonly used to alleviate the effect of noise on high-dimensional distances, such as for spectral clustering [Liu and Han, 2004], biological cell trajectory inference [Street et al., 2018, Saelens et al., 2019, Vandaele et al., 2020, Vandaele et al., 2021] (Figure 1), and even prior to other embedding methods such as t-SNE [Van der Maaten and Hinton, 2008]. However,

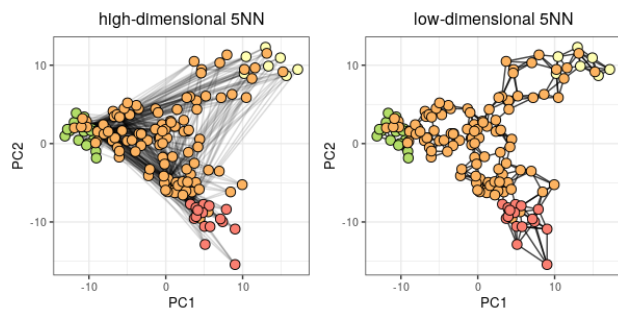


Figure 1: 5NN graphs (edges in black) of a real bifurcating biological cell trajectory (gene expression) data set $\mathbf{X} + \mathbf{N} \subseteq \mathbb{R}^{1770}$ consisting of four cell groups [Cannoodt et al., 2018, Saelens et al., 2019, Vandaele et al., 2020]. Each dimension corresponds to the expression of a particular gene, and the coloring of each point (cell) on the plots corresponds to its cell group. The 5NN graphs are visualized through a 2-dimensional PCA embedding of $\mathbf{X} + \mathbf{N}$. (Left) The edges of the 5NN graph are obtained directly from the distances between the high-dimensional points. (Right) The edges of the 5NN graph are obtained from the 2-dimensional PCA embedding. The possible placement of points is much more constrained in the 2-dimensional plane. This reduces unwanted behavior caused by high-dimensional noisy distances, such as noisy interconnections between different branches, which impedes trajectory inference. The resulting lower-dimensional representation will be more effective for learning the bifurcating model, as common in cell trajectory inference [Saelens et al., 2019].

a formal exploration of how these themselves are susceptible to noise in high dimensions—as we provide in this paper—is lacking. While we only study this empirically for a synthetic example within the limited scope of this paper, the fact that *our derived phase shift where neighbors become random or not is identical to the phase shift where common dimensionality reductions methods perform poorly or well*, encourages further theoretical and methodological research into this subject.

2 Quantifying the effect of noise on high-dimensional neighbors

In the first part of this section (Section 2.1), we provide a probabilistic quantification of the effect of noise on the absolute discrimination between high-dimensional neighbors (Theorem 2.1), and use this to deduce conditions under which empirical neighbors become either highly random or highly effective (Corollary 2.3). In particular, it will follow that these conditions are independent of the magnitude of noise in the dimensions. While we commence our analysis assuming we have three fixed points $\mathbf{x}, \mathbf{y}, \mathbf{z} \in \mathbf{X}$ in a given ground truth data set \mathbf{X} , in Section 2.2 we also discuss how our obtained results can be used to derive more general results for \mathbf{X} , such as Theorem 2.6.

2.1 When neighbors become (non-)random: a case study for three points

Our setting in this section will be as follows.

- We are given three sequences (vectors) $\mathbf{x} = x_1, x_2, \dots$, $\mathbf{y} = y_1, y_2, \dots$, and $\mathbf{z} = z_1, z_2, \dots$. These correspond to our ground truth—and thus in practice—non-observed points. For $d \in \mathbb{N}^*$, x_d equals the information captured by the d -th dimension of \mathbf{x} (analogous for \mathbf{y}, \mathbf{z}). In the case that our model is explained by a finite number of dimensions, we can still regard $\mathbf{x}, \mathbf{y}, \mathbf{z}$ as infinite sequences by letting $x_d = y_d = z_d$ for irrelevant dimensions d .
- Rather than observing $\mathbf{x}, \mathbf{y}, \mathbf{z}$, we observe $\mathbf{x} + \mathbf{n}_x, \mathbf{y} + \mathbf{n}_y, \mathbf{z} + \mathbf{n}_z$. Here, \mathbf{n}_x is a realization of a sequence of random noise variables $\mathbf{n}_x = n_{x_1}, n_{x_2}, \dots$ (analogous for \mathbf{y}, \mathbf{z}). We will assume the random variables to be i.i.d., have finite fourth moment μ'_4 (measuring the heaviness of the tail of the noise distribution), and be symmetric. While the former two assumptions will be required by our analysis, the latter simply makes it more. Nevertheless, many common random noise distributions such as uniform and normal, are symmetric.

The result below should be interpreted as follows. We are given a query point \mathbf{x} from a ground truth data set \mathbf{X} , and two candidate neighbors \mathbf{y} and \mathbf{z} . We want a formula expressing how likely neighborhood relations between \mathbf{x}, \mathbf{y} , and \mathbf{z} , such as ‘ \mathbf{x} is closer to \mathbf{y} than to \mathbf{z} ’, are preserved after introducing additive noise \mathbf{N} , i.e., we observe $\mathbf{X} + \mathbf{N}$ rather than \mathbf{X} . This formula should be asymptotically valid, i.e., for a sufficiently high dimensionality d of \mathbf{X} . Intuitively, the resulting probabilities will be in terms of the true distances $\|\mathbf{x} - \mathbf{y}\|$ and $\|\mathbf{x} - \mathbf{z}\|$, and noise characteristics, in our case σ^2 and μ'_4 . Indeed, when there is not much difference between $\|\mathbf{x} - \mathbf{y}\|$ and $\|\mathbf{x} - \mathbf{z}\|$ (the signal), or when σ^2 and μ'_4 are large, we expect it to be more difficult to preserve the neighborhood relations. The following formula will then be used to derive subsequent insightful results.

Theorem 2.1. *Let $\mathbf{x} = x_1, x_2, \dots$, $\mathbf{y} = y_1, y_2, \dots$ and $\mathbf{z} = z_1, z_2, \dots$ be three sequences of reals. Let $\mathbf{n}_x = n_{x_1}, n_{x_2}, \dots$, $\mathbf{n}_y = n_{y_1}, n_{y_2}, \dots$, and $\mathbf{n}_z = n_{z_1}, n_{z_2}, \dots$ be three sequences of jointly i.i.d. symmetric continuous random variables with variance σ^2 and finite 4th moment μ'_4 . For a sequence \mathbf{s} , denote $\mathbf{s}^{(d)}$ for the vector composed from its first d elements in order. Finally, let*

$$\Delta_\infty(d) := \max \left\{ \left\| \mathbf{x}^{(d)} - \mathbf{y}^{(d)} \right\|_\infty, \left\| \mathbf{x}^{(d)} - \mathbf{z}^{(d)} \right\|_\infty \right\}.$$

If

$$\lim_{d \rightarrow \infty} \frac{\Delta_\infty(d)}{\sqrt{d}} = 0, \quad (1)$$

then

$$\left| P \left(\left\| \mathbf{x}^{(d)} + \mathbf{n}_x^{(d)} - \mathbf{y}^{(d)} - \mathbf{n}_y^{(d)} \right\| \leq \left\| \mathbf{x}^{(d)} + \mathbf{n}_x^{(d)} - \mathbf{z}^{(d)} - \mathbf{n}_z^{(d)} \right\| \right) - \Phi \left(\zeta^{(d)}(\mu'_4, \sigma, \mathbf{x}, \mathbf{y}, \mathbf{z}) \right) \right| \xrightarrow{d \rightarrow \infty} 0,$$

where

$$\begin{aligned} \zeta^{(d)} : (\mathbb{R}^+)^2 \times (\mathbb{R}^d)^3 &\rightarrow \mathbb{R} : (\mu'_4, \sigma, \mathbf{x}, \mathbf{y}, \mathbf{z}) \\ &\mapsto \frac{\|\mathbf{x} - \mathbf{z}\|^2 - \|\mathbf{x} - \mathbf{y}\|^2}{\sqrt{2d(\mu'_4 + 3\sigma^4) + 8\sigma^2(\|\mathbf{x} - \mathbf{y}\|^2 + \|\mathbf{x} - \mathbf{z}\|^2 - \langle \mathbf{x} - \mathbf{y}, \mathbf{x} - \mathbf{z} \rangle)}}, \end{aligned} \quad (2)$$

and Φ is the cumulative distribution function of the standard normal distribution.

Letting

$$\begin{aligned} z^{(d)} &:= \left\| \mathbf{n}_x^{(d)} - \mathbf{n}_y^{(d)} + \mathbf{x}^{(d)} - \mathbf{y}^{(d)} \right\|^2 \\ &\quad - \left\| \mathbf{n}_x^{(d)} - \mathbf{n}_z^{(d)} + \mathbf{x}^{(d)} - \mathbf{z}^{(d)} \right\|^2 \\ &= \sum_{i=1}^d \underbrace{\left[(n_{x_i} - n_{y_i} + x_i - y_i)^2 - (n_{x_i} - n_{z_i} + x_i - z_i)^2 \right]}_{=: z_i}, \end{aligned} \quad (3)$$

the proof of Theorem 2.1 is based on an application of the central limit theorem (CLT) to quantify the limiting behavior of $z(d)$. However, the random variables z_i , $i = 1, \dots, d$, are not necessarily identically distributed, i.e., with the same mean and variance. Unlike the analysis by [Beyer et al., 1999, Aggarwal et al., 2001], we thus need special conditions to ensure that the CLT is applicable. To this end, (1) provides a sufficient condition for Linderberg’s condition to be satisfied [Lindeberg, 1922]. A proof of Theorem 2.1 is given in Appendix B.

Remark 2.2. *Following our proof in Appendix B, condition (1) can be further weakened to either one of the following conditions:*

$$\left(\frac{\Delta_\infty^4(d)}{d + \|\mathbf{x}^{(d)} - \mathbf{y}^{(d)}\| \|\mathbf{x}^{(d)} - \mathbf{z}^{(d)}\|} \xrightarrow{d \rightarrow \infty} 0 \right) \wedge \left(\frac{\min\{d\Delta_\infty^4(d), \|\mathbf{x}^{(d)} - \mathbf{y}^{(d)}\|^2 \|\mathbf{x}^{(d)} - \mathbf{z}^{(d)}\|^2\}}{(d + \|\mathbf{x}^{(d)} - \mathbf{y}^{(d)}\| \|\mathbf{x}^{(d)} - \mathbf{z}^{(d)}\|)^{\frac{5}{4}}} \xrightarrow{d \rightarrow \infty} 0 \right), \quad (4)$$

or

$$\left(\frac{\Delta_\infty^4(d)}{d + \|\mathbf{x}^{(d)} - \mathbf{y}^{(d)}\| \|\mathbf{x}^{(d)} - \mathbf{z}^{(d)}\|} \xrightarrow{d \rightarrow \infty} 0 \right) \wedge (\forall \epsilon > 0) \left(\frac{F_n \left(- \left(d + \|\mathbf{x}^{(d)} - \mathbf{y}^{(d)}\| \|\mathbf{x}^{(d)} - \mathbf{z}^{(d)}\| \right)^{\frac{1}{4}} \epsilon \right) \times \min\{d\Delta_\infty^4(d), \|\mathbf{x}^{(d)} - \mathbf{y}^{(d)}\|^2 \|\mathbf{x}^{(d)} - \mathbf{z}^{(d)}\|^2\}}{d + \|\mathbf{x}^{(d)} - \mathbf{y}^{(d)}\| \|\mathbf{x}^{(d)} - \mathbf{z}^{(d)}\|} \xrightarrow{d \rightarrow \infty} 0 \right), \quad (5)$$

where F_n is the cumulative distribution function of our (marginal) random noise variable \mathbf{n} . Using Markov’s inequality, it can be straightforwardly shown that (1) \implies (4) \implies (5). While these conditions are less insightful than (1), condition (5) can e.g. be used to easily show that it suffices that $\Delta_\infty(d) = o\left(d^{\frac{1}{4}}\right)$ in the generic case that \mathbf{n} is bounded. Nevertheless, in the practical case that $\Delta_\infty(d)$ is bounded, i.e., when newly added dimensions are (eventually) at most as discriminating as the former, condition (1) is trivially satisfied. In the Corollary 2.3 we will assume such bound, as it allows for a convenient way to ‘symmetrize’ our asymptotic growth conditions in this result.

Under the same setting as for Theorem 2.1, i.e., given a query point \mathbf{x} and two candidate neighbors \mathbf{y} and \mathbf{z} , we can now study growth conditions on the signal—this being how well we can discriminate between \mathbf{y} and \mathbf{z} as the ground truth neighbors of \mathbf{x} —under which the signal ‘beats’ the noise in high dimensions and vice versa. If the noise beats the signal, then the empirical neighborhood relations, i.e., those derived after additive noise is introduced—thus from our actual measured data—will be (nearly) completely random. This is expressed by Corollary 2.3.1 below. In the opposite case, the signal beats the noise, and the empirical neighborhood relations will (likely) agree with those

that would be derived without noise, i.e., from the ground truth. This is expressed by Corollary 2.3.2. The proofs of these results are provided in Appendix B.

Corollary 2.3. *Let $\mathbf{x} = x_1, x_2, \dots$, $\mathbf{y} = y_1, y_2, \dots$ and $\mathbf{z} = z_1, z_2, \dots$ be three sequences of reals. Let $\mathbf{n}_\mathbf{x} = n_{x_1}, n_{x_2}, \dots$, $\mathbf{n}_\mathbf{y} = n_{y_1}, n_{y_2}, \dots$, and $\mathbf{n}_\mathbf{z} = n_{z_1}, n_{z_2}, \dots$ be three sequences of jointly i.i.d. symmetric continuous random variables with finite 4th moment μ_4' . Suppose further that $\sup_{d \in \mathbb{N}^*} \Delta_\infty(d) \leq C$ for some $C > 0$. Then the following statements are true.*

$$1. \text{ If } \|\mathbf{x}^{(d)} - \mathbf{z}^{(d)}\|^2 - \|\mathbf{x}^{(d)} - \mathbf{y}^{(d)}\|^2 = o\left(d^{\frac{1}{2}}\right),$$

$$\lim_{d \rightarrow \infty} P \left(\left\| \mathbf{x}^{(d)} + \mathbf{n}_\mathbf{x}^{(d)} - \mathbf{y}^{(d)} - \mathbf{n}_\mathbf{y}^{(d)} \right\| \leq \left\| \mathbf{x}^{(d)} + \mathbf{n}_\mathbf{x}^{(d)} - \mathbf{z}^{(d)} - \mathbf{n}_\mathbf{z}^{(d)} \right\| \right) = \frac{1}{2}.$$

$$2. \text{ If } d^{\frac{1}{2}} = o\left(\|\mathbf{x}^{(d)} - \mathbf{z}^{(d)}\|^2 - \|\mathbf{x}^{(d)} - \mathbf{y}^{(d)}\|^2\right),$$

$$\lim_{d \rightarrow \infty} P \left(\left\| \mathbf{x}^{(d)} + \mathbf{n}_\mathbf{x}^{(d)} - \mathbf{y}^{(d)} - \mathbf{n}_\mathbf{y}^{(d)} \right\| \leq \left\| \mathbf{x}^{(d)} + \mathbf{n}_\mathbf{x}^{(d)} - \mathbf{z}^{(d)} - \mathbf{n}_\mathbf{z}^{(d)} \right\| \right) = 1.$$

Remark 2.4. *The following conclusions—which will be validated in Section 3—can now be made.*

1. $\max\{\|\mathbf{x}^{(d)} - \mathbf{y}^{(d)}\|, \|\mathbf{x}^{(d)} - \mathbf{z}^{(d)}\|\}$ should grow at least as $d^{\frac{1}{4}}$, otherwise neighbors will become random. Indeed, if we would have $\max\{\|\mathbf{x}^{(d)} - \mathbf{y}^{(d)}\|, \|\mathbf{x}^{(d)} - \mathbf{z}^{(d)}\|\} = o\left(d^{\frac{1}{4}}\right)$, then condition (5) is satisfied, and Corollary 2.3.1 becomes applicable (note that the bound $\sup_{d \in \mathbb{N}^*} \Delta_\infty(d) \leq C$ is only required for Corollary 2.3.2).

2. Whereas the noise characteristics σ^2 and μ_4' naturally have a direct effect on the usefulness of empirical neighbors for any fixed dimension d —as can also be seen from (2)—under the conditions of Corollary 2.3, their magnitude becomes negligible in limiting dimensions.

3. Even if the distances between the noise vectors largely determine the distances between the observed data points, neighbors may become non-random, i.e., representative for the ground truth neighbors. E.g., if the random noise variable \mathbf{n} is uniformly distributed, then the expected distances between two noise vectors grows as \sqrt{d} , whereas it is sufficient for the absolute differences between ground truth distances to grow as $\sqrt[4]{d} + \epsilon$ for some $\epsilon > 0$ to ensure that the noise becomes unlikely to effect neighbors in sufficiently high dimensions.

The following example will prove very useful in our experiments (Section 3).

Example 2.5. Let $\mathbf{x} = \mathbf{y}$ be the sequences of all zeros. Given $\alpha \in \mathbb{R}_{>2} \cup \{\infty\}$, we define the sequence $\mathbf{z}(\alpha) = z_1(\alpha), z_2(\alpha), \dots$ by letting for $i \in \mathbb{N}^*$,

$$z_i(\alpha) := \begin{cases} \frac{1}{\sqrt{i}} & \text{if } \alpha \in \mathbb{R}_{>2}; \\ 1 & \text{if } \alpha = \infty. \end{cases}$$

Observe that $\Delta_\infty(d) = \|\mathbf{z}^{(d)}(\alpha)\|_\infty = 1$ for all $d \in \mathbb{N}^*$. We furthermore find that for $\alpha \in \mathbb{R}_{>2}$, $\|\mathbf{z}^{(d)}(\alpha)\|^2$ defines a hyperharmonic series, which for large $d \in \mathbb{N}^*$ can be approximated as

$$\|\mathbf{z}^{(d)}(\alpha)\|^2 = \sum_{i=1}^d \frac{1}{\alpha \sqrt{i^2}} \stackrel{d \rightarrow \infty}{\sim} \int_1^d x^{-\frac{2}{\alpha}} dx = \left(\frac{\alpha}{\alpha-2}\right) \left(d^{1-\frac{2}{\alpha}} - 1\right), \quad (6)$$

i.e., $\|\mathbf{z}^{(d)}(\alpha)\|^2$ grows as $d^{1-\frac{2}{\alpha}}$. With by convention $\frac{1}{\infty} = 0$, this holds for $\alpha = \infty$ as well. Naturally, in any dimension \mathbf{y} is always closer to \mathbf{x} than \mathbf{z} is. Due to Corollary 2.3, the probability that this remains true under noise in high dimensions satisfies

$$P\left(\|\mathbf{x}^{(d)} + \mathbf{n}_{\mathbf{x}}^{(d)} - \mathbf{y}^{(d)} - \mathbf{n}_{\mathbf{y}}^{(d)}\| \leq \|\mathbf{x}^{(d)} + \mathbf{n}_{\mathbf{x}}^{(d)} - \mathbf{z}^{(d)} - \mathbf{n}_{\mathbf{z}}^{(d)}\|\right) \stackrel{d \rightarrow \infty}{\rightarrow} \begin{cases} \frac{1}{2} & \alpha < 4; \\ 1 & \alpha > 4; \\ \Phi\left(\sqrt{\frac{2}{\mu_4 + 3\sigma^4}}\right) & \alpha = 4. \end{cases}$$

The last limit can be found through (6) by adapting our proof of Corollary 2.3.2 in Appendix B.

In the following section, we discuss how our obtained results can now be used to derive more general results for larger data sets \mathbf{X} , i.e., consisting of more than three points \mathbf{x} , \mathbf{y} , and \mathbf{z} .

2.2 Randomness in neighbors for data sets of arbitrary sizes

In the previous section we restricted to the particular scenario where we have three given points \mathbf{x} , \mathbf{y} , and \mathbf{z} . Naturally, we can also study the effectiveness of deriving neighborhood relations in a data set \mathbf{X} of arbitrary size under the effect of noise in high dimensions. The reason for this is that in practice, we deal with a finite number of data points. Therefore, more general mathematical results on preserving neighbors under noise may often be derived directly from our results in Section 2.1.

One such example is as follows, providing sufficient growth conditions on the ground truth diameter for the noise to cause neighboring relations to become random, or thus necessary conditions for the noise not to cause this (which is what we want to achieve in

practice). The idea here is that when for every point $\mathbf{x} \in \mathbf{X}$, if its true furthest neighbor becomes closer to it than its true closest neighbor—according to our empirical noisy data—is completely random, i.e., this occurs with probability $\frac{1}{2}$, then one can essentially not effectively work with the high-dimensional neighbors.

Theorem 2.6. Let $\mathbf{X} = \mathbf{v}_1, \mathbf{v}_2, \dots$ be a sequence of column vectors, for which $\mathbf{v}_d \in \mathbb{R}^n$, $n \in \mathbb{N}^*$, and denote by $\mathbf{X}^{(d)}$ the matrix in $\mathbb{R}^{n \times d}$ composed of the first d vectors \mathbf{v}_d in order. For $d \in \mathbb{N}^*$, and $i = 1, \dots, n$, we identify the i -th row of the matrix $\mathbf{X}^{(d)}$ with the point $\mathbf{x}_i^{(d)} \in \mathbf{X}^{(d)}$. Let furthermore $\{\mathbf{n}_i = n_{i_1}, n_{i_2}, \dots\}_{i \in \{1, \dots, n\}}$ be a collection of jointly i.i.d. symmetric continuous random variables with finite 4th moment. For $d \in \mathbb{N}^*$ and each point $\mathbf{x}_i^{(d)} \in \mathbf{X}^{(d)}$, let $\mathbf{x}_{i,\min}^{(d)}$ denote the closest neighbor of $\mathbf{x}_i^{(d)}$ in $\mathbf{X}^{(d)}$, $\mathbf{x}_{i,\max}^{(d)}$ the furthest neighbor of $\mathbf{x}_i^{(d)}$ in $\mathbf{X}^{(d)}$, and $\Delta_2(\mathbf{d}) := \max_{\mathbf{x}, \mathbf{y} \in \mathbf{X}^{(d)}} \|\mathbf{x} - \mathbf{y}\|$ the diameter of $\mathbf{X}^{(d)}$. If $\Delta_2(\mathbf{d}) = \mathbf{o}\left(d^{\frac{1}{4}}\right)$, then

$$\sup_{i=1, \dots, n} P\left(\left\|\mathbf{x}_i^{(d)} + \mathbf{n}_i^{(d)} - \mathbf{x}_{i,\max}^{(d)} - \mathbf{n}_{\mathbf{x}_{i,\max}^{(d)}}^{(d)}\right\| \leq \left\|\mathbf{x}_i^{(d)} + \mathbf{n}_i^{(d)} - \mathbf{x}_{i,\min}^{(d)} - \mathbf{n}_{\mathbf{x}_{i,\min}^{(d)}}^{(d)}\right\|\right) \stackrel{d \rightarrow \infty}{\rightarrow} \frac{1}{2}. \quad (7)$$

Proof. Corollary 2.3.1 is valid for every triple of rows in \mathbf{X} (see also Remark 2.4.1). Hence, the result follows from the fact that there are only finitely many such triples (note that the row indices of $\mathbf{x}_{i,\min}^{(d)}$ and $\mathbf{x}_{i,\max}^{(d)}$ in $\mathbf{X}^{(d)}$ are allowed to vary with d). \square

Theorem 2.6 essentially states the conditions we should definitely avoid for any application that relies on the proximity of data observations. Conversely, the conditions we should aim for are generally more dependant on the application of interest. Indeed, for many practical purposes it may not be important to preserve *all* neighborhood relations in the data. E.g., in clustering it may not be necessary to preserve them within the same cluster, but rather between clusters. Different clustering linkage criteria may also lead to different conditions that need to be satisfied. Hence—although conditions for such cases may be derived from Corollary 2.3.2—we will not claim one such generally applicable result. Nevertheless, the consensus remains that to overcome the impact of the extra noise, adding extra dimensions should ideally be accompanied with adding sufficient information to discriminate between important neighbors according to the ground truth.

3 Experimental results

In this section, we will conduct experiments that aim to increase ones understanding and intuition

about working with high-dimensional noisy distances. First, Section 3.1 will be devoted to empirical validation of our theoretical results. Section 3.2 will be devoted to linking the performance of common dimensionality reduction methods to randomness of neighborhood relations. All code for this project is available on dropbox.com/sh/f467nglenzt8ue0/AADFSxboz9qvFV8ytQ32JHCEa?dl=0.

3.1 Validation of our theoretical results

We will focus on validating Corollary 2.3 and the conclusions that can be made from this result (Remark 2.4). A separate validation of Theorem 2.1 is included in Appendix A.

Validation of Corollary 2.3 We will use Example 2.5 to assess the existence of an exact growth rate of the true discrimination between neighbors for which empirical neighbors become random or not. For this, we considered various sets of three sequences \mathbf{x} , \mathbf{y} , and \mathbf{z} , where $\mathbf{x} = \mathbf{y}$, and $\mathbf{z} = \mathbf{z}(\alpha)$ controls the growth rate as determined by α in Example 2.5. We sampled noise using a uniform distribution $\mathbf{n} \sim U[-1.25, 1.25]$.¹ A relatively high magnitude of noise is chosen to better illustrate that $0 < \Phi_4 := \Phi\left(\sqrt{\frac{2}{\mu_4^2 + 3\sigma^4}}\right) < 1$ (for $\alpha \neq 4$ the magnitude will not matter in the limit). The setup of this experiment is visualized through Figure 2. We used 5000 noise replicates to approximate a variety of expected values and probabilities for different growth rates determined by $\alpha \in \{2, 3, 4, 5, 6, \infty\}$. These are illustrated on Figure 3, and defined as follows.

1. The expected distance between two noise vectors, compared to the ground truth diameter growth rates, i.e., of $\|\mathbf{z}\|$ (Figure 3, Left).
2. The expected *relative contrast* (Figure 3, Middle) [Aggarwal et al., 2001]:

$$\frac{\max_{\mathbf{p}, \mathbf{q} \in \{\mathbf{x}, \mathbf{y}, \mathbf{z}\}} \|\mathbf{p} + \mathbf{n}_p - \mathbf{q} - \mathbf{n}_q\|}{\min_{\mathbf{p}, \mathbf{q} \in \{\mathbf{x}, \mathbf{y}, \mathbf{z}\}} \|\mathbf{p} + \mathbf{n}_p - \mathbf{q} - \mathbf{n}_q\|} - 1.$$

A relative contrast near 0 indicates distance concentration (Section 1).

3. The probability (Figure 3, Right)

$$P(\|\mathbf{x} + \mathbf{n}_x - \mathbf{y} - \mathbf{n}_y\| \leq \|\mathbf{x} + \mathbf{n}_x - \mathbf{z} - \mathbf{n}_z\|).$$

First, we observe that the distances between the noise vectors is expected to become indefinitely larger than

¹We empirically validated all results in this section for Gaussian distributions as well. Note that exact the type of distribution does not matter, as long as the conditions for our theoretical result of interest are met.

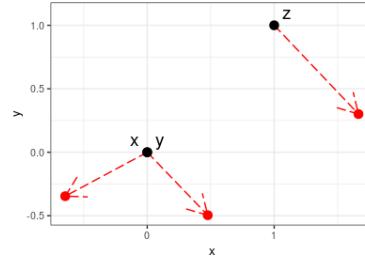


Figure 2: The setup for our experiment visualized in 2D. We have three points $\mathbf{x} = \mathbf{y}$ and \mathbf{z} , where \mathbf{z} controls our true discrimination growth rate. Theorem 2.1 can be used to quantify how likely \mathbf{x} will remain closer to \mathbf{y} than to \mathbf{z} under the effect of noise in high dimensions, here illustrated by the displacements in red, for various growth rates.

the distances between the ground truth points for $\alpha < \infty$ (Figure 3, Left). Hence, we would anticipate the distances between the noise vectors to play a dominant role in our observed empirical distances for the corresponding growth rates. Second, we observe that for also all considered growth rates specified by $\alpha < \infty$, the expected relative contrast converges to 0 (Figure 3, Middle). This means that in sufficiently high dimensions, the two closest points are expected to be relatively as distant to each other as the two furthest points. If one would interpret this as neighborhood queries to become meaningless and unstable—as argued by [Beyer et al., 1999, Aggarwal et al., 2001]—according to our notion discussed in Section 1, this should result in a lot of randomness in the chosen

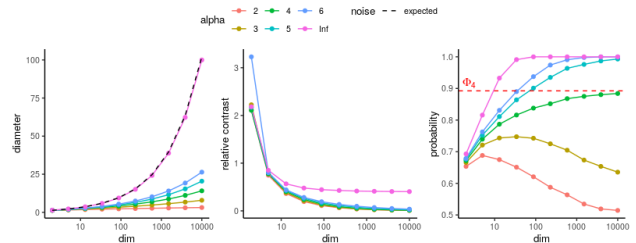


Figure 3: (Left) The expected growth rate of the distance between two noise vectors compared to the ground truth model diameter growth rates determined by α . (Middle) The expected relative contrast converges to 0 for all considered values $\alpha \neq \infty$, meaning that the two closest points are expected to be relatively as distant to each other as the two furthest points. (Right) The limiting behavior of $P(\|\mathbf{x} + \mathbf{n}_x - \mathbf{y} - \mathbf{n}_y\| \leq \|\mathbf{x} + \mathbf{n}_x - \mathbf{z} - \mathbf{n}_z\|)$. Under high-dimensional noise, neighbors will be inferred effectively for $\alpha > 4$, i.e., empirical neighbors will likely be true, whereas for $\alpha < 4$, they become meaningless.

closest neighbor of the noisy observation representing \mathbf{x} in the high-dimensional space for all considered $\alpha \in \{2, \dots, 6\}$. However, as discussed Example 2.5, this will not hold whenever $\alpha > 4$, as \mathbf{x} will be very likely to correctly choose \mathbf{y} as its neighbor even when this decision is affected by noise in high dimensions. This is confirmed by our empirical probabilities (Figure 3, Right), which furthermore agree with all limits obtained in Example 2.5 from Corollary 2.3.

3.2 Dimensionality reduction with random neighbors

As discussed in Section 1, dimensionality reductions are commonly applied for preprocessing high-dimensional noisy data. The obtained distances in the lower-dimensional space are commonly more effective for inference and machine learning. This raises the question whether dimensionality reductions can naturally accommodate for the effect of noise on high-dimensional neighboring relations.

To investigate this, consider a ground truth data set \mathbf{X} of n evenly spaced points on the line segment \mathcal{L} from the origin to $\mathbf{z}^{(d)}$ in \mathbb{R}^d , where $\mathbf{z} = \mathbf{z}(\alpha)$ is as defined in Example 2.5 by fixing some $\alpha \in \mathbb{R}_{>2} \cup \{\infty\}$ (Figure 4, Left). Since these points are evenly spaced on \mathcal{L} , the growth rate of all squared distances (and the differences between them) will be identical to the growth rate of $\|\mathbf{z}^{(d)}\|^2$, up to some constant factor depending on the fixed ground truth ordering of the considered points. Thus, from Corollary 2.3 we find that under the effect of noise in high dimensions, *all* empirical neighbors will become random for $\alpha < 4$, and *all* empirical neighbors will likely be true for $\alpha > 4$.

For a 1D-dimensionality reduction method f , we can study how well f is able to recover neighboring relations of \mathbf{X} from $\mathbf{X} + \mathbf{N}$, with \mathbf{N} a random noise matrix, through the correlation between the ordering of points on \mathbf{X} and on $f(\mathbf{X} + \mathbf{N})$ (Figure

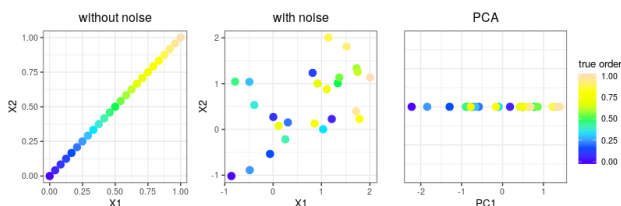


Figure 4: (Left) $n = 25$ ground truth points \mathbf{X} are evenly spaced on a linear model $L \subseteq \mathbb{R}^d$. (Middle) Rather than observing \mathbf{X} , we observe $\mathbf{X} + \mathbf{N}$ for some random noise matrix \mathbf{N} . (Right) A 1-dimensional PCA dimensionality reduction aims to retrieve the true ordering of points on L .

4). To this end, we apply six different dimensionality reduction methods that are commonly used for noise or feature size reduction prior to visualization, (topological) inference, or clustering: PCA [Wold et al., 1987, Van der Maaten and Hinton, 2008, Street et al., 2018, Cannoodt et al., 2016], UMAP [McInnes et al., 2018], diffusion maps [Coifman and Lafon, 2006, Vandaele et al., 2020, Cannoodt et al., 2016], robust PCA [Candès et al., 2011] (a variant of PCA that assumes the data is composed in a low-rank component X and a *sparse* noise component N), a basic autoencoder [Kramer, 1991, Vincent et al., 2010] with 5 hidden layers and tanh activation, and Isomap [Tenenbaum et al., 2000]. We evaluated their performances for $n = 25$ points, up to $d = 10\,000$ dimensions, growth rates determined by $\alpha \in \{2, 3, 4, 5, 6, \infty\}$, and averaged over 100 noise replicates from a uniform noise distribution $n \sim U[-1.25, 1.25]$ per dimension. The autoencoder was built in Python. Other models ran under standard settings in R (changing the number of neighbors from 50 to 10 for Isomap). The results are shown in Figure 5.

We consistently observe that the performances increase by dimension for $\alpha > 4$, and decrease for $\alpha < 4$. Following our previous results (Figure 3, Right), this thus provides empirical evidence that the performance of these common dimensionality reduction methods is directly affected by whether noise causes randomness in high-dimensional neighborhood relations or not, thus concluding that they themselves may be susceptible to the noise they aim to reduce. These observations are only contradicted by the autoencoder, which showed convergence issues for larger dimensions.

Finally, the case $\alpha = 4$ deserves special interest. Since

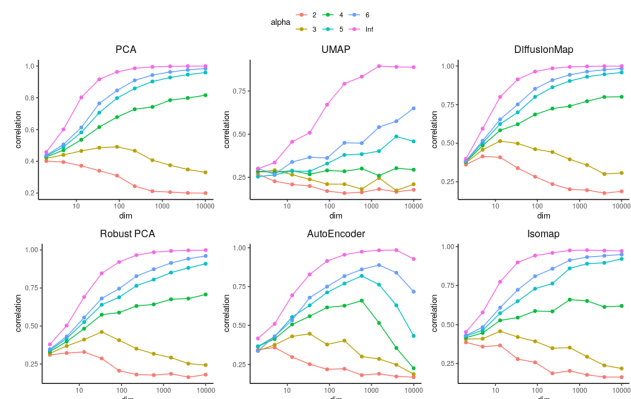


Figure 5: The performance of six common dimensionality reduction methods for recovering the ground truth ordering of the points on L under the effect of noise, by dimension and growth rate.

in a practical setting additional distributional conditions of \mathbf{X} will likely result in some non-extreme degree of randomness in empirical neighbors, we observe that this may be reflected in the performance of dimensionality reductions as well.

Note that while these results are unfavorable for dimensionality reductions, we focused on one small artificial data set. *We empirically observed that for larger data sets, we also required larger dimensions to show the limiting behavior of the dimensionality reduction performances for $\alpha < 4$. Thus, in practice—and as common in machine learning applications—having more data can resolve much of the issues caused by noise.* Intuitively, the dimension at which we are unable to effectively recover our model gets delayed for larger data sizes. This may explain why dimensionality reductions are often still successfully applied in point cloud representation learning to reduce the effect of the noise in the high-dimensional space, and facilitate consecutive learning and inference. The results in this paper highly encourage further theoretical and practical research into this subject.

4 Discussion and conclusion

Noise can be, but must not be, fatal when learning from high-dimensional data based on similarities. Although this is not a surprising fact, we provided a first and exact mathematical characterization when such similarities become (un)informative under noise. Furthermore, we found that our concept of meaningfulness of distances—when they are informative for the ground truth—is fundamentally different from distance concentration, and suggests direct connections to the ability of dimensionality reductions to recover the data model. Although we focused on small artificial data sets to validate the results in this (mainly theoretical) paper, they are interesting nevertheless, and encourage further foundational and practical research into high-dimensional noisy point cloud representation learning.

Unfortunately, our conditions for distances to be meaningful will be difficult to assess in practice. For example, one can easily derive from our results that when many features are irrelevant to our model, neighborhood relations will be uninformative in the presence of noise. In practice however, we may be unsure whether any features are irrelevant at all. How algorithms may actually benefit from the results presented in this paper, is open to further research. Nevertheless, such work will undoubtedly have high impact, as there is an abundance of high-dimensional data where we cannot effectively recover the structure due to noise, leading to poor subsequent model inference, such as in biological single-cell data analysis. Better

understanding the behavior of distances in noisy high-dimensional data—for which we provided, illustrated, and validated theoretical results in this paper—is imperative for one to be able to design better computational methods for their analysis.

Acknowledgments

Use unnumbered third level headings for the acknowledgments. All acknowledgments, including those to funding agencies, go at the end of the paper.

References

- [Aggarwal et al., 2001] Aggarwal, C. C., Hinneburg, A., and Keim, D. A. (2001). On the surprising behavior of distance metrics in high dimensional space. In Van den Bussche, J. and Vianu, V., editors, *Database Theory — ICDT 2001*, pages 420–434, Berlin, Heidelberg. Springer Berlin Heidelberg.
- [Beyer et al., 1999] Beyer, K., Goldstein, J., Ramakrishnan, R., and Shaft, U. (1999). When is “nearest neighbor” meaningful? In *International conference on database theory*, pages 217–235. Springer.
- [Buades et al., 2005] Buades, A., Coll, B., and Morel, J.-M. (2005). A non-local algorithm for image denoising. In *2005 IEEE Computer Society Conference on Computer Vision and Pattern Recognition (CVPR’05)*, volume 2, pages 60–65. IEEE.
- [Candès et al., 2011] Candès, E. J., Li, X., Ma, Y., and Wright, J. (2011). Robust principal component analysis? *Journal of the ACM (JACM)*, 58(3):1–37.
- [Cannoodt et al., 2016] Cannoodt, R., Saelens, W., and Saeys, Y. (2016). Computational methods for trajectory inference from single-cell transcriptomics. *European journal of immunology*, 46(11):2496–2506.
- [Cannoodt et al., 2018] Cannoodt, R., Saelens, W., Todorov, H., and Saeys, Y. (2018). Single-cell -omics datasets containing a trajectory.
- [Coifman and Lafon, 2006] Coifman, R. R. and Lafon, S. (2006). Diffusion maps. *Applied and computational harmonic analysis*, 21(1):5–30.
- [Durrant and Kabán, 2009] Durrant, R. J. and Kabán, A. (2009). When is ‘nearest neighbour’ meaningful: A converse theorem and implications. *Journal of Complexity*, 25(4):385–397.
- [Ertöz et al., 2003] Ertöz, L., Steinbach, M., and Kumar, V. (2003). Finding clusters of different sizes, shapes, and densities in noisy, high dimensional data. In *Proceedings of the 2003 SIAM international conference on data mining*, pages 47–58. SIAM.

- [Giannella, 2021] Giannella, C. R. (2021). Instability results for euclidean distance, nearest neighbor search on high dimensional gaussian data. *Information Processing Letters*, 169:106115.
- [Indyk and Motwani, 1998] Indyk, P. and Motwani, R. (1998). Approximate nearest neighbors: towards removing the curse of dimensionality. In *Proceedings of the thirtieth annual ACM symposium on Theory of computing*, pages 604–613.
- [Kabán, 2012] Kabán, A. (2012). Non-parametric detection of meaningless distances in high dimensional data. *Statistics and Computing*, 22(2):375–385.
- [Kramer, 1991] Kramer, M. A. (1991). Nonlinear principal component analysis using autoassociative neural networks. *AIChE journal*, 37(2):233–243.
- [Kuo and Sloan, 2005] Kuo, F. Y. and Sloan, I. H. (2005). Lifting the curse of dimensionality. *Notices of the AMS*, 52(11):1320–1328.
- [Libralon et al., 2009] Libralon, G. L., de Leon Ferreira, A. C. P., Lorena, A. C., et al. (2009). Pre-processing for noise detection in gene expression classification data. *Journal of the Brazilian Computer Society*, 15(1):3–11.
- [Lindeberg, 1922] Lindeberg, J. W. (1922). Eine neue herleitung des exponentialgesetzes in der wahrscheinlichkeitsrechnung. *Mathematische Zeitschrift*, 15(1):211–225.
- [Liu and Han, 2004] Liu, J. and Han, J. (2004). Spectral clustering. *Advances in neural information processing systems*, 17:1601–1608.
- [McInnes et al., 2018] McInnes, L., Healy, J., and Melville, J. (2018). Umap: Uniform manifold approximation and projection for dimension reduction. *arXiv preprint arXiv:1802.03426*.
- [Radovanović et al., 2009] Radovanović, M., Nanopoulos, A., and Ivanović, M. (2009). Nearest neighbors in high-dimensional data: The emergence and influence of hubs. In *Proceedings of the 26th Annual International Conference on Machine Learning, ICML '09*, pages 865–872, New York, NY, USA. ACM.
- [Saelens et al., 2019] Saelens, W., Cannoodt, R., Todorov, H., and Saeys, Y. (2019). A comparison of single-cell trajectory inference methods. *Nature Biotechnology*, 37:1.
- [Street et al., 2018] Street, K., Risso, D., Fletcher, R., Das, D., Ngai, J., Yosef, N., Purdom, E., and Dudoit, S. (2018). Slingshot: Cell lineage and pseudo-time inference for single-cell transcriptomics. *BMC Genomics*, 19.
- [Tenenbaum et al., 2000] Tenenbaum, J. B., De Silva, V., and Langford, J. C. (2000). A global geometric framework for nonlinear dimensionality reduction. *science*, 290(5500):2319–2323.
- [Van der Maaten and Hinton, 2008] Van der Maaten, L. and Hinton, G. (2008). Visualizing data using t-sne. *Journal of machine learning research*, 9(11).
- [Vandaele et al., 2021] Vandaele, R., Rieck, B., Saeys, Y., and De Bie, T. (2021). Stable topological signatures for metric trees through graph approximations. *Pattern Recognition Letters*.
- [Vandaele et al., 2020] Vandaele, R., Saeys, Y., and Bie, T. D. (2020). Mining topological structure in graphs through forest representations. *Journal of Machine Learning Research*, 21(215):1–68.
- [Verleysen and François, 2005] Verleysen, M. and François, D. (2005). The curse of dimensionality in data mining and time series prediction. In *International work-conference on artificial neural networks*, pages 758–770. Springer.
- [Vincent et al., 2010] Vincent, P., Larochelle, H., Larjoie, I., Bengio, Y., Manzagol, P.-A., and Bottou, L. (2010). Stacked denoising autoencoders: Learning useful representations in a deep network with a local denoising criterion. *Journal of machine learning research*, 11(12).
- [Wold et al., 1987] Wold, S., Esbensen, K., and Geladi, P. (1987). Principal component analysis. *Chemometrics and intelligent laboratory systems*, 2(1-3):37–52.
- [Zhang et al., 2021] Zhang, R., Atwal, G. S., and Lim, W. K. (2021). Noise regularization removes correlation artifacts in single-cell rna-seq data preprocessing. *Patterns*, 2(3):100211.
- [Zhu and Wu, 2004] Zhu, X. and Wu, X. (2004). Class noise vs. attribute noise: A quantitative study. *Artificial intelligence review*, 22(3):177–210.

A Supplementary experiments

This section of the Appendix contains additional experiments to verify the correctness of our theoretical results provided in the main paper.

Validation of Theorem 2.1 We constructed three sets of three different sequences \mathbf{x} , \mathbf{y} , and \mathbf{z} containing up to 10 000 dimensions. For each set, we let $\mathbf{x} = \mathbf{y}$ be the sequences of all zeros, while \mathbf{z} is used to control our ground truth growth rates, here of the l_2 and l_∞ norm, as follows.

- l_2 bounded, l_∞ bounded:

$$\mathbf{z} = (1, 0, \dots, 0).$$

- l_2 unbounded, l_∞ bounded:

$$\mathbf{z} = (1, 1, \dots, 1).$$

- l_2 unbounded, l_∞ unbounded:

$$\mathbf{z} = \left(d^{\frac{1}{4}-\epsilon} \right)_{d=1, \dots, 10\,000}, \text{ with } \epsilon = 0.01.$$

Then for each sequence and in each dimension we added uniform noise $n \sim U[-0.75, 0.75]$, for which $\sigma^2 = \frac{0.75^2}{3}$ and $\mu_4' = \frac{0.75^4}{5}$. The setup for this experiment is thus also illustrated by Figure 2 in the main paper. Since n is bounded in each dimension, Theorem 2.1 should be applicable to all three cases (see also Remark 2.2). More precisely, for sufficiently large d we should find that $y(d) := \frac{z(d) - \mu(z(d))}{\sigma(z(d))} \overset{\text{approx.}}{\sim} N(0, 1)$, where $z(d)$ is as defined in (3), and $\mu(z(d))$ is the negative nominator and $\sigma(z(d))$ the denominator of $\zeta^{(d)}(\mu_4', \sigma, \mathbf{x}, \mathbf{y}, \mathbf{z})$ in (2). We verified this by obtaining 5000 samples of $y(d)$ for each of the ground truth growth rates and various dimension d chosen from a log-scale (replicating the noise outcomes), and conducted the Shapiro–Wilk test to assess normality. The results are shown in Figure 6, confirming that Theorem 2.1 is indeed applicable to all of our considered growth rates. Since the Shapiro–Wilk test is developed to assess normality, but not *standard* normality, Figures 7 and 8 show normality plots of $y(d)$ for $d = 2$ and $d = 10\,000$, respectively, for the second set of sequences, confirming the correctness of our calculations.

B Theorems and proofs

This section of the Appendix contains the mathematical proofs of our results presented in the main paper. First, we require the following lemma that states that convergence in probability of continuous random variables implies uniform convergence in the cumulative distribution functions.

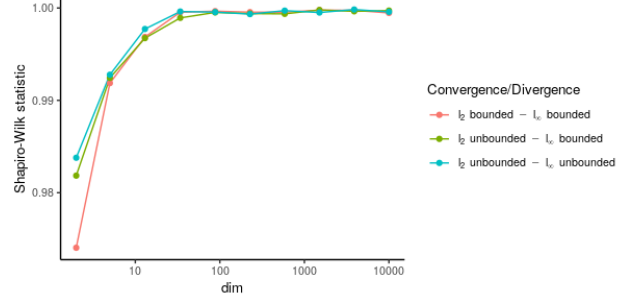


Figure 6: Shapiro–Wilk test statistics to assess normality of $y(d)$ for the various growth rates determined by \mathbf{z} , according to the dimension of the ground truth points \mathbf{x} , \mathbf{y} , and \mathbf{z} . The convergence of the curves to 1 agrees that Theorem 2.1 is applicable to all of our growth rates, and thus allows us to quantify the randomness of neighborhood relations between \mathbf{x} , \mathbf{y} , and \mathbf{z} caused by noise.

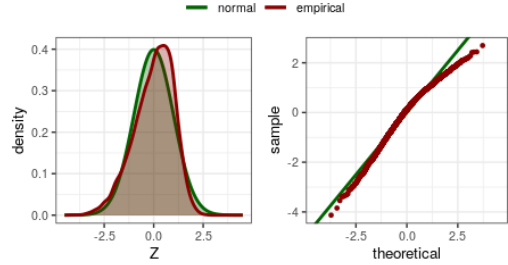


Figure 7: Density plot and Q–Q plot of $y(2)$ (empirical) compared to the standard normal distribution.

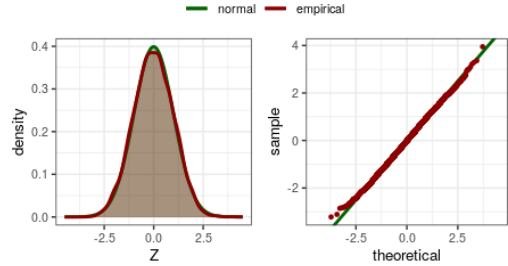


Figure 8: Density plot and Q–Q plot of $y(10\,000)$ (empirical) compared to the standard normal distribution.

Lemma B.1. *Let x_1, x_2, \dots , be a sequence of random variables for which $x_n \xrightarrow[n \rightarrow \infty]{p} x$ for some continuous random variable x . Then*

$$\lim_{n \rightarrow \infty} \sup_{t \in \mathbb{R}} |P(x_n \leq t) - P(x \leq t)| = 0.$$

Proof. By assumption, $F_{x_n}(t) = P(x_n \leq t) \xrightarrow[n \rightarrow \infty]{p} P(x \leq t) = F_x(t)$ for every continuity point t of F_x , and thus every $t \in \mathbb{R}$. Hence, it suffices to show that this convergence is uniform. Being a bounded, monotonically increasing, continuous function, F_x itself is

uniformly continuous on \mathbb{R} . Since $\lim_{t \rightarrow -\infty} F_x(t) = 0$, and $\lim_{t \rightarrow +\infty} F_x(t) = 1$, for any ϵ , we can thus find

$$t_1 < t_2 < \dots < t_{k-1} < t_k,$$

such that $F_x(t_i) - F_x(t_{i-1}) \leq \epsilon$, $i = 2, \dots, k$, $F_x(t_1) \leq \epsilon$, $F_x(t_k) \geq 1 - \epsilon$. Now assume n is sufficiently large such that $|F_{x_n}(t_i) - F_x(t_i)| \leq \epsilon$ for all $i = 1, \dots, k$, and arbitrarily take $t \in \mathbb{R}$. There now exists t_i , $i = 0, \dots, k$, such that $t \in [t_i, t_{i+1}]$, where by convention $t_0 = -\infty$, $F_x(t_0) = 0$, and $t_{k+1} = +\infty$, $F_x(t_{k+1}) = 1$. We then have

$$\begin{aligned} |F_{x_n}(t) - F_x(t)| &\leq |F_{x_n}(t) - F_{x_n}(t_i)| \\ &\quad + |F_{x_n}(t_i) - F_x(t_i)| \\ &\quad + |F_x(t_i) - F_x(t)| \\ &\leq |F_{x_n}(t_{i+1}) - F_{x_n}(t_i)| + 2\epsilon \\ &\leq |F_{x_n}(t_{i+1}) - F_x(t_{i+1})| \\ &\quad + |F_x(t_{i+1}) - F_x(t_i)| \\ &\quad + |F_x(t_i) - F_{x_n}(t_i)| + 2\epsilon \\ &\leq 5\epsilon. \end{aligned}$$

This shows that F_{x_n} converges uniformly to F_x . \square

We are now ready to provide the proof leading to the principal results in our main paper.

Proof of Theorem 2.1. For $i \in \mathbb{N}^*$, denote $\delta_i(\mathbf{x}, \mathbf{y}) := x_i - y_i$ and $\delta_i(\mathbf{x}, \mathbf{z}) := x_i - z_i$. For each $d \in \mathbb{N}^*$, we have

$$\begin{aligned} z(d) &:= \left\| \mathbf{n}_{\mathbf{x}}^{(d)} - \mathbf{n}_{\mathbf{y}}^{(d)} + \mathbf{x}^{(d)} - \mathbf{y}^{(d)} \right\|^2 - \left\| \mathbf{n}_{\mathbf{x}}^{(d)} - \mathbf{n}_{\mathbf{z}}^{(d)} + \mathbf{x}^{(d)} - \mathbf{z}^{(d)} \right\|^2 \\ &= \sum_{i=1}^d \left[\underbrace{\left(\underbrace{n_{x_i} - n_{y_i} + \delta_i(\mathbf{x}, \mathbf{y})}_{=: r_{x_i, y_i}} \right)^2}_{=: z_i} - \underbrace{\left(\underbrace{n_{x_i} - n_{z_i} + \delta_i(\mathbf{x}, \mathbf{z})}_{=: r_{x_i, z_i}} \right)^2}_{=: z_i} \right]. \end{aligned}$$

We have

$$\mathbb{E}(r_{x_i, y_i}) = \delta_i(\mathbf{x}, \mathbf{y}), \quad \text{Var}(r_{x_i, y_i}) = 2\sigma^2,$$

so that

$$\mathbb{E}(r_{x_i, y_i}^2) = \text{Var}(r_{x_i, y_i}) + \mathbb{E}(r_{x_i, y_i})^2 = 2\sigma^2 + \delta_i^2(\mathbf{x}, \mathbf{y}),$$

and thus

$$\mathbb{E}(z_i) = \delta_i^2(\mathbf{x}, \mathbf{y}) - \delta_i^2(\mathbf{x}, \mathbf{z}).$$

Since $\text{Cov}(\mathbf{x}, \mathbf{y}) = \mathbb{E}(\mathbf{x}\mathbf{y}) - \mathbb{E}(\mathbf{x})\mathbb{E}(\mathbf{y})$ for random variables \mathbf{x}, \mathbf{y} , by symmetry and the fact that n_{x_i} and n_{y_i} are independent and $\mathbb{E}(n_{x_i}^{2k+1}) = 0$ for $k \in \mathbb{N}$, we have

$$\begin{aligned} \text{Var}(r_{x_i, y_i}^2) &= 2\text{Var}(n_{x_i}^2) - 8\text{Cov}(n_{x_i}^2, n_{x_i}n_{y_i}) \\ &\quad + 4\text{Var}(n_{x_i}n_{y_i}) + 8\delta_i^2(x, y)\text{Var}(n_{x_i}) \\ &= 2\left(\mu'_4 - \mathbb{E}(n_{x_i}^2)^2\right) + 4\mathbb{E}(n_{x_i}^2)^2 \\ &\quad + 8\sigma^2\delta_i^2(\mathbf{x}, \mathbf{y}) \\ &= 2\mu'_4 + 2\sigma^4 + 8\sigma^2\delta_i^2(\mathbf{x}, \mathbf{y}) \end{aligned}$$

and analogously

$$\begin{aligned} \text{Cov}(r_{x_i, y_i}^2, r_{x_i, z_i}^2) &= \text{Var}(n_{x_i}^2) \\ &\quad - 4\text{Cov}(n_{x_i}^2, n_{x_i}n_{y_i}) \\ &\quad + 2(\delta_i(\mathbf{x}, \mathbf{y}) + \delta_i(\mathbf{x}, \mathbf{z}))\text{Cov}(n_{x_i}^2, n_{x_i}) \\ &\quad + 4\text{Cov}(n_{x_i}n_{y_i}, n_{x_i}n_{z_i}) \\ &\quad - 4(\delta_i(\mathbf{x}, \mathbf{y}) + \delta_i(\mathbf{x}, \mathbf{z}))\text{Cov}(n_{x_i}n_{y_i}, n_{x_i}) \\ &\quad + 4\delta_i(\mathbf{x}, \mathbf{y})\delta_i(\mathbf{x}, \mathbf{z})\text{Var}(n_{x_i}) \\ &= \mu'_4 - \mathbb{E}(n_{x_i}^2)^2 + 4\sigma^2\delta_i(\mathbf{x}, \mathbf{y})\delta_i(\mathbf{x}, \mathbf{z}) \\ &= \mu'_4 - \sigma^4 + 4\sigma^2\delta_i(\mathbf{x}, \mathbf{y})\delta_i(\mathbf{x}, \mathbf{z}). \end{aligned}$$

It thus holds that

$$\begin{aligned} \text{Var}(z_i) &= \text{Var}(r_{x_i, y_i}^2) + \text{Var}(r_{x_i, z_i}^2) \\ &\quad - 2\text{Cov}(r_{x_i, y_i}^2, r_{x_i, z_i}^2) \\ &= 2\mu'_4 + 6\sigma^4 \\ &\quad + 8\sigma^2(\delta_i^2(\mathbf{x}, \mathbf{y}) + \delta_i^2(\mathbf{x}, \mathbf{z}) - \delta_i(\mathbf{x}, \mathbf{y})\delta_i(\mathbf{x}, \mathbf{z})). \end{aligned}$$

We conclude that

$$\mu(z(d)) = \sum_{i=1}^d \mathbb{E}(z_i) = \left\| \mathbf{x}^{(d)} - \mathbf{y}^{(d)} \right\|^2 - \left\| \mathbf{x}^{(d)} - \mathbf{z}^{(d)} \right\|^2,$$

and

$$\begin{aligned} \sigma^2(z(d)) &= \sum_{i=1}^d \text{Var}(z_i) \\ &= 2d(\mu'_4 + 3\sigma^4) \\ &\quad + 8\sigma^2 \left(\left\| \mathbf{x}^{(d)} - \mathbf{y}^{(d)} \right\|^2 + \left\| \mathbf{x}^{(d)} - \mathbf{z}^{(d)} \right\|^2 \right. \\ &\quad \left. - \left\langle \mathbf{x}^{(d)} - \mathbf{y}^{(d)}, \mathbf{x}^{(d)} - \mathbf{z}^{(d)} \right\rangle \right). \end{aligned}$$

Also observe that

$$\begin{aligned} &\left\| \mathbf{x}^{(d)} - \mathbf{y}^{(d)} \right\|^2 + \left\| \mathbf{x}^{(d)} - \mathbf{z}^{(d)} \right\|^2 \\ &\quad - \left\langle \mathbf{x}^{(d)} - \mathbf{y}^{(d)}, \mathbf{x}^{(d)} - \mathbf{z}^{(d)} \right\rangle \\ &\geq \left\| \mathbf{x}^{(d)} - \mathbf{y}^{(d)} \right\|^2 + \left\| \mathbf{x}^{(d)} - \mathbf{z}^{(d)} \right\|^2 \\ &\quad - \left\| \mathbf{x}^{(d)} - \mathbf{y}^{(d)} \right\| \left\| \mathbf{x}^{(d)} - \mathbf{z}^{(d)} \right\| \\ &= \left(\left\| \mathbf{x}^{(d)} - \mathbf{y}^{(d)} \right\| - \left\| \mathbf{x}^{(d)} - \mathbf{z}^{(d)} \right\| \right)^2 \\ &\quad + \left\| \mathbf{x}^{(d)} - \mathbf{y}^{(d)} \right\| \left\| \mathbf{x}^{(d)} - \mathbf{z}^{(d)} \right\| \\ &\geq \left\| \mathbf{x}^{(d)} - \mathbf{y}^{(d)} \right\| \left\| \mathbf{x}^{(d)} - \mathbf{z}^{(d)} \right\|, \end{aligned}$$

which is used for Remark 2.2 in the main paper. Now for $\epsilon > 0$, let

$$\mathbb{A}_{i, \epsilon} := \{(n_{x_i}, n_{y_i}, n_{z_i}) : |z_i - \mathbb{E}(z_i)| > \epsilon\sigma(z(d))\},$$

and

$$C_d(\epsilon) := \frac{1}{12} \left(\sqrt{\underbrace{36\Delta_\infty^2(d) + 24\epsilon\sigma(z(d))}_{=:D}} - 6\Delta_\infty(d) \right).$$

For any $\epsilon > 0$ and $M \geq \sqrt{\frac{6}{\epsilon}}$, by (1), we find that for d sufficiently large

$$\begin{aligned} C_d(\epsilon) &\geq \frac{\sqrt{24\epsilon} - \frac{6}{M}}{12} \sqrt{\sigma(z(d))} \\ &\geq \frac{2\sqrt{6\epsilon} - \sqrt{6\epsilon}}{12} \sqrt{\sigma(z(d))} = \frac{\sqrt{6\epsilon}}{12} \sqrt{\sigma(z(d))}, \end{aligned} \quad (8)$$

so that in particular $\lim_{d \rightarrow \infty} C_d(\epsilon) = +\infty$. If now

$$\max\{|n_{x_i}|, |n_{y_i}|, |n_{z_i}|\} \leq C_d(\epsilon),$$

we find that for $i = 1, \dots, d$,

$$\begin{aligned} |z_i - \mathbb{E}(z_i)| &\leq |n_{y_i}|^2 + |n_{z_i}|^2 + 2|n_{x_i}||n_{y_i}| + 2|n_{x_i}||n_{z_i}| \\ &\quad + 2(|n_{x_i}| + |n_{y_i}| + |n_{z_i}|)\Delta_\infty(d) \\ &\leq 6C_d(\epsilon)^2 + 6\Delta_\infty(d)C_d(\epsilon) \\ &\leq \frac{1}{24} \left(72\Delta_\infty^2(d) + 24\epsilon\sigma(z(d)) - 12\Delta_\infty(d)\sqrt{D} \right) \\ &\quad + \frac{1}{2} \left(\Delta_\infty(d)\sqrt{D} - 6\Delta_\infty^2(d) \right) \\ &= \epsilon\sigma(z(d)). \end{aligned}$$

This shows that

$$\begin{aligned} \mathbb{A}_{i,\epsilon} &\subseteq \{(n_{x_i}, n_{y_i}, n_{z_i}) : \max\{|n_{x_i}|, |n_{y_i}|, |n_{z_i}|\} > C_d(\epsilon)\} \\ &=: \tilde{\mathbb{A}}_{i,\epsilon}. \end{aligned}$$

Observe that for every $i, k, l \in \mathbb{N}^*$, we have

$$\begin{aligned} &\mathbb{E} \left(n_{x_i}^{2k+1} n_{y_i}^l \mathbb{1}_{\tilde{\mathbb{A}}_{i,\epsilon}} \right) \\ &= \mathbb{E} \left(n_{x_i}^{2k+1} \right) \mathbb{E} \left(n_{y_i}^l \right) \\ &\quad - \mathbb{E} \left(n_{x_i}^{2k+1} \mathbb{1}_{(\tilde{\mathbb{A}}_{i,\epsilon})^c} \right) \mathbb{E} \left(n_{y_i}^l \mathbb{1}_{(\tilde{\mathbb{A}}_{i,\epsilon})^c} \right) \\ &= 0. \end{aligned}$$

Again, due to symmetry, we thus have

$$\begin{aligned} &\mathbb{E} \left((r_{x_i, y_i}^2 - r_{x_i, z_i}^2) \mathbb{1}_{\tilde{\mathbb{A}}_{i,\epsilon}} \right) \\ &= (\delta_i^2(\mathbf{x}, \mathbf{y}) - \delta_i^2(\mathbf{x}, \mathbf{z})) P \left(\tilde{\mathbb{A}}_{i,\epsilon} \right). \end{aligned}$$

Furthermore, we have

$$\begin{aligned} \mathbb{E} \left(r_{x_i, y_i}^4 \mathbb{1}_{\tilde{\mathbb{A}}_{i,\epsilon}} \right) &= 2\mathbb{E} \left(n_{x_i}^4 \mathbb{1}_{\tilde{\mathbb{A}}_{i,\epsilon}} \right) + 6\mathbb{E} \left(n_{x_i}^2 n_{y_i}^2 \mathbb{1}_{\tilde{\mathbb{A}}_{i,\epsilon}} \right) \\ &\quad + 12\delta_i^2(\mathbf{x}, \mathbf{y}) \mathbb{E} \left(n_{x_i}^2 \mathbb{1}_{\tilde{\mathbb{A}}_{i,\epsilon}} \right) + \\ &\quad \delta_i(\mathbf{x}, \mathbf{y})^4 P \left(\tilde{\mathbb{A}}_{i,\epsilon} \right), \end{aligned}$$

and

$$\begin{aligned} &\mathbb{E} \left((r_{x_i, y_i}^2 r_{x_i, z_i}^2) \mathbb{1}_{\tilde{\mathbb{A}}_{i,\epsilon}} \right) \\ &= \mathbb{E} \left(n_{x_i}^4 \mathbb{1}_{\tilde{\mathbb{A}}_{i,\epsilon}} \right) + 3\mathbb{E} \left(n_{x_i}^2 n_{y_i}^2 \mathbb{1}_{\tilde{\mathbb{A}}_{i,\epsilon}} \right) \\ &\quad + 2(\delta_i(\mathbf{x}, \mathbf{y}) + \delta_i(\mathbf{x}, \mathbf{z}))^2 \mathbb{E} \left(n_{x_i}^2 \mathbb{1}_{\tilde{\mathbb{A}}_{i,\epsilon}} \right) \\ &\quad + \delta_i(\mathbf{x}, \mathbf{y})^2 \delta_i(\mathbf{x}, \mathbf{z})^2 P \left(\tilde{\mathbb{A}}_{i,\epsilon} \right). \end{aligned}$$

Putting things together, we have

$$\begin{aligned} &\mathbb{E} \left((z_i - \mathbb{E}(z_i))^2 \mathbb{1}_{\mathbb{A}_{i,\epsilon}} \right) \\ &\leq \mathbb{E} \left((z_i - \mathbb{E}(z_i))^2 \mathbb{1}_{\tilde{\mathbb{A}}_{i,\epsilon}} \right) \\ &= \mathbb{E} \left((r_{x_i, y_i}^2 - r_{x_i, z_i}^2)^2 \mathbb{1}_{\tilde{\mathbb{A}}_{i,\epsilon}} \right) \\ &\quad - 2\mathbb{E}(x_i) \mathbb{E} \left((r_{x_i, y_i}^2 - r_{x_i, z_i}^2) \mathbb{1}_{\tilde{\mathbb{A}}_{i,\epsilon}} \right) + \mathbb{E}(z_i)^2 P \left(\tilde{\mathbb{A}}_{i,\epsilon} \right) \\ &= \mathbb{E} \left(r_{x_i, y_i}^4 \mathbb{1}_{\tilde{\mathbb{A}}_{i,\epsilon}} \right) + \mathbb{E} \left(r_{x_i, z_i}^4 \mathbb{1}_{\tilde{\mathbb{A}}_{i,\epsilon}} \right) \\ &\quad - 2\mathbb{E} \left((r_{x_i, y_i}^2 r_{x_i, z_i}^2) \mathbb{1}_{\tilde{\mathbb{A}}_{i,\epsilon}} \right) \\ &\quad + \mathbb{E}(z_i) P \left(\tilde{\mathbb{A}}_{i,\epsilon} \right) \left(\mathbb{E}(z_i) - 2(\delta_i^2(\mathbf{x}, \mathbf{y}) - \delta_i^2(\mathbf{x}, \mathbf{z})) \right) \\ &= 2\mathbb{E} \left(n_{x_i}^4 \mathbb{1}_{\tilde{\mathbb{A}}_{i,\epsilon}} \right) + 6\mathbb{E} \left(n_{x_i}^2 n_{y_i}^2 \mathbb{1}_{\tilde{\mathbb{A}}_{i,\epsilon}} \right) \\ &\quad + 8(\delta_i^2(\mathbf{x}, \mathbf{y}) + \delta_i^2(\mathbf{x}, \mathbf{z}) - \delta_i(\mathbf{x}, \mathbf{y})\delta_i(\mathbf{x}, \mathbf{z})) \\ &\quad \quad \quad \times \mathbb{E} \left(n_{x_i}^2 \mathbb{1}_{\tilde{\mathbb{A}}_{i,\epsilon}} \right) \\ &\quad + \delta_i^2(\mathbf{x}, \mathbf{y})\delta_i^2(\mathbf{x}, \mathbf{z}) P \left(\tilde{\mathbb{A}}_{i,\epsilon} \right). \end{aligned}$$

Now since for each $j, k, l \in \mathbb{N}$, it holds that

$$\begin{aligned} &\mathbb{E} \left(n_{x_i}^{2j} n_{y_i}^{2k} n_{z_i}^{2l} \mathbb{1}_{\tilde{\mathbb{A}}_{i,\epsilon}} \right) \\ &\leq \mathbb{E} \left(n_{x_i}^{2j} \mathbb{1}_{|n_{x_i}| > C_d(\epsilon)} \right) \mathbb{E} \left(n_{y_i}^{2k} \right) \mathbb{E} \left(n_{z_i}^{2l} \right) \\ &\quad + \mathbb{E} \left(n_{y_i}^{2k} \mathbb{1}_{|n_{y_i}| > C_d(\epsilon)} \right) \mathbb{E} \left(n_{x_i}^{2j} \right) \mathbb{E} \left(n_{z_i}^{2l} \right) \\ &\quad + \mathbb{E} \left(n_{z_i}^{2l} \mathbb{1}_{|n_{z_i}| > C_d(\epsilon)} \right) \mathbb{E} \left(n_{x_i}^{2j} \right) \mathbb{E} \left(n_{y_i}^{2k} \right), \end{aligned}$$

we find that

$$\begin{aligned} &\mathbb{E} \left((z_i - \mathbb{E}(z_i))^2 \mathbb{1}_{\mathbb{A}_{i,\epsilon}} \right) \\ &\leq 2 \left(\mathbb{E} \left(n_{x_i}^4 \mathbb{1}_{|n_{x_i}| > C_d(\epsilon)} \right) + 2\mu'_4 P(|n_{x_i}| > C_d(\epsilon)) \right) \\ &\quad + 6 \left(2\sigma^2 \mathbb{E} \left(n_{x_i}^2 \mathbb{1}_{|n_{x_i}| > C_d(\epsilon)} \right) + \sigma^4 P(|n_{x_i}| > C_d(\epsilon)) \right) \\ &\quad + 8(\delta_i^2(\mathbf{x}, \mathbf{y}) + \delta_i^2(\mathbf{x}, \mathbf{z}) - \delta_i(\mathbf{x}, \mathbf{y})\delta_i(\mathbf{x}, \mathbf{z})) \\ &\quad \quad \quad \times \left(\mathbb{E} \left(n_{x_i}^2 \mathbb{1}_{|n_{x_i}| > C_d(\epsilon)} \right) + 2\sigma^2 P(|n_{x_i}| > C_d(\epsilon)) \right) \\ &\quad + 3\delta_i^2(\mathbf{x}, \mathbf{y})\delta_i^2(\mathbf{x}, \mathbf{z}) P(|n_{x_i}| > C_d(\epsilon)) \\ &\leq 2\mathbb{E} \left(n_{x_i}^4 \mathbb{1}_{|n_{x_i}| > C_d(\epsilon)} \right) + 12\sigma^2 \mathbb{E} \left(n_{x_i}^2 \mathbb{1}_{|n_{x_i}| > C_d(\epsilon)} \right) \\ &\quad + 8(\delta_i^2(\mathbf{x}, \mathbf{y}) + \delta_i^2(\mathbf{x}, \mathbf{z}) - \delta_i(\mathbf{x}, \mathbf{y})\delta_i(\mathbf{x}, \mathbf{z})) \\ &\quad \quad \quad \times \mathbb{E} \left(n_{x_i}^2 \mathbb{1}_{|n_{x_i}| > C_d(\epsilon)} \right) \\ &\quad + (4\mu'_4 + 6\sigma^4 + 16 \max\{1, \sigma^2\} M_i) P(|n_{x_i}| > C_d(\epsilon)), \end{aligned}$$

where

$$M_i := \delta_i^2(\mathbf{x}, \mathbf{y}) + \delta_i^2(\mathbf{x}, \mathbf{z}) - \delta_i(\mathbf{x}, \mathbf{y})\delta_i(\mathbf{x}, \mathbf{z}) \\ + \delta_i^2(\mathbf{x}, \mathbf{y})\delta_i^2(\mathbf{x}, \mathbf{z}).$$

Summing over $i = 1, \dots, d$, we find that

$$\frac{1}{\sigma^2(\mathbf{z}(d))} \sum_{i=1}^d \mathbb{E} \left(\mathbf{n}_{x_i}^4 \mathbb{1}_{|\mathbf{n}_{x_i}| > C_d(\epsilon)} \right) \\ \leq \frac{d \mathbb{E} \left(\mathbf{n}_{x_1}^4 \mathbb{1}_{|\mathbf{n}_{x_1}| > C_d(\epsilon)} \right)}{\sigma^2(2d(\mu'_4 + 3\sigma^4))} \xrightarrow{d \rightarrow \infty} 0,$$

since μ'_4 is finite and $C_d(\epsilon) \xrightarrow{d \rightarrow \infty} +\infty$. Analogously, we have

$$\frac{1}{\sigma^2(\mathbf{z}(d))} \sum_{i=1}^d \mathbb{E} \left(\mathbf{n}_{x_i}^2 \mathbb{1}_{|\mathbf{n}_{x_i}| > C_d(\epsilon)} \right) \xrightarrow{d \rightarrow \infty} 0.$$

We also have

$$\frac{1}{\sigma^2(\mathbf{z}(d))} \sum_{i=1}^d (\delta_i^2(\mathbf{x}, \mathbf{y}) + \delta_i^2(\mathbf{x}, \mathbf{z}) - \delta_i(\mathbf{x}, \mathbf{y})\delta_i(\mathbf{x}, \mathbf{z})) \\ \times \mathbb{E} \left(\mathbf{n}_{x_i}^2 \mathbb{1}_{|\mathbf{n}_{x_i}| > C_d(\epsilon)} \right) \\ \leq \frac{1}{8\sigma^2} \mathbb{E} \left(\mathbf{n}_{x_1}^2 \mathbb{1}_{|\mathbf{n}_{x_1}| > C_d(\epsilon)} \right) \xrightarrow{d \rightarrow \infty} 0.$$

Finally, we have that

$$\frac{1}{\sigma^2(\mathbf{z}(d))} \sum_{i=1}^d M_i P(|\mathbf{n}_{x_i}| > C_d(\epsilon)) \xrightarrow{d \rightarrow \infty} 0.$$

Indeed, given our observation above, it suffices to show that

$$P(|\mathbf{n}_{x_1}| > C_d(\epsilon)) \frac{\sum_{i=1}^d \delta_i^2(\mathbf{x}, \mathbf{y})\delta_i^2(\mathbf{x}, \mathbf{z})}{\sigma^2(\mathbf{z}(d))} \xrightarrow{d \rightarrow \infty} 0.$$

Using Markov's inequality, (1), and (8), this follows from the fact that for d sufficiently large

$$P(|\mathbf{n}_{x_1}| > C_d(\epsilon)) \frac{\sum_{i=1}^d \delta_i^2(\mathbf{x}, \mathbf{y})\delta_i^2(\mathbf{x}, \mathbf{z})}{\sigma^2(\mathbf{z}(d))} \\ \leq \frac{\mathbb{E}(|\mathbf{n}_{x_1}|) d \Delta_\infty^4(d)}{C_d(\epsilon) \sigma^2(\mathbf{z}(d))} \\ \leq \frac{12 \mathbb{E}(|\mathbf{n}_{x_1}|) d \Delta_\infty^4(d)}{\sqrt{6} \epsilon \sigma^{\frac{5}{2}}(\mathbf{z}(d))} \xrightarrow{d \rightarrow \infty} 0.$$

We conclude that

$$\lim_{d \rightarrow \infty} \frac{1}{\sigma^2(\mathbf{z}(d))} \mathbb{E} \left((z_i - \mathbb{E}(z_i))^2 \mathbb{1}_{\mathbb{A}_{i,\epsilon}} \right) = 0,$$

and this for every $\epsilon > 0$. Hence, Linderberg's condition is satisfied, so that we may apply the central limit theorem to $\mathbf{z}(d)$, i.e.,

$$\frac{\mathbf{z}(d) - \mu(\mathbf{z}(d))}{\sigma(\mathbf{z}(d))} \xrightarrow{d \rightarrow \infty} \mathcal{N}(0, 1).$$

Hence, from Lemma B.1, we find that

$$\lim_{d \rightarrow \infty} \left| P(\mathbf{z}(d) \leq 0) - \Phi \left(-\frac{\mu(\mathbf{z}(d))}{\sigma(\mathbf{z}(d))} \right) \right| \\ = \lim_{d \rightarrow \infty} \left| P \left(\frac{\mathbf{z}(d) - \mu(\mathbf{z}(d))}{\sigma(\mathbf{z}(d))} \leq -\frac{\mu(\mathbf{z}(d))}{\sigma(\mathbf{z}(d))} \right) \right. \\ \left. - \Phi \left(-\frac{\mu(\mathbf{z}(d))}{\sigma(\mathbf{z}(d))} \right) \right| = 0,$$

which concludes the proof. \square

Theorem 2.1 can now be used to easily derive Corollary 2.3 as follows.

Proof of Corollary 2.3. 1. This is an immediate consequence of Theorem 2.1.

2. By assumption, it holds that

$$\frac{d}{\left(\|\mathbf{x}^{(d)} - \mathbf{z}^{(d)}\|^2 - \|\mathbf{x}^{(d)} - \mathbf{y}^{(d)}\|^2 \right)^2} \xrightarrow{d \rightarrow \infty} 0.$$

Furthermore, we have

$$0 \leq \frac{\|\mathbf{x}^{(d)} - \mathbf{y}^{(d)}\|^2 + \|\mathbf{x}^{(d)} - \mathbf{z}^{(d)}\|^2 - \langle \mathbf{x}^{(d)} - \mathbf{y}^{(d)}, \mathbf{x}^{(d)} - \mathbf{z}^{(d)} \rangle}{\left(\|\mathbf{x}^{(d)} - \mathbf{z}^{(d)}\|^2 - \|\mathbf{x}^{(d)} - \mathbf{y}^{(d)}\|^2 \right)^2} \\ \leq \frac{\left(\|\mathbf{x}^{(d)} - \mathbf{y}^{(d)}\| + \|\mathbf{x}^{(d)} - \mathbf{z}^{(d)}\| \right)^2}{\left(\|\mathbf{x}^{(d)} - \mathbf{z}^{(d)}\| - \|\mathbf{x}^{(d)} - \mathbf{y}^{(d)}\| \right)^2} \\ \times \left(\|\mathbf{x}^{(d)} - \mathbf{z}^{(d)}\| + \|\mathbf{x}^{(d)} - \mathbf{y}^{(d)}\| \right)^2 \\ = \frac{1}{\left(\|\mathbf{x}^{(d)} - \mathbf{z}^{(d)}\| - \|\mathbf{x}^{(d)} - \mathbf{y}^{(d)}\| \right)^2}.$$

Now choose any $M > 0$. We know that for d sufficiently large

$$\left\| \mathbf{x}^{(d)} - \mathbf{z}^{(d)} \right\| - \left\| \mathbf{x}^{(d)} - \mathbf{y}^{(d)} \right\| \\ = \frac{\left\| \mathbf{x}^{(d)} - \mathbf{z}^{(d)} \right\|^2 - \left\| \mathbf{x}^{(d)} - \mathbf{y}^{(d)} \right\|^2}{\left\| \mathbf{x}^{(d)} - \mathbf{z}^{(d)} \right\| + \left\| \mathbf{x}^{(d)} - \mathbf{y}^{(d)} \right\|} \\ \geq \frac{2MC\sqrt{d}}{2\Delta_\infty(d)\sqrt{d}} \geq M,$$

so that $\frac{1}{\left(\|\mathbf{x}^{(d)} - \mathbf{z}^{(d)}\| - \|\mathbf{x}^{(d)} - \mathbf{y}^{(d)}\| \right)^2} \xrightarrow{d \rightarrow \infty} 0$. Hence, $\zeta^{(d)}(\mu'_4, \sigma, \mathbf{x}^{(d)}, \mathbf{y}^{(d)}, \mathbf{z}^{(d)}) \xrightarrow{d \rightarrow \infty} \infty$. The result now follows from Theorem 2.1. \square